

# Melting of monolayer protected cluster superlattices

N. Sandhyarani

*Department of Chemistry and Regional Sophisticated Instrumentation Centre,  
Indian Institute of Technology, Madras 600 036, India*

M. P. Antony and G. Panneer Selvam

*Radiochemistry Laboratory, Indira Gandhi Centre for Atomic Research, Kalpakkam, Tamil Nadu, India*

T. Pradeep<sup>a)</sup>

*Department of Chemistry and Regional Sophisticated Instrumentation Centre,  
Indian Institute of Technology, Madras 600 036, India*

(Received 20 June 2000; accepted 11 September 2000)

Melting of crystalline solids (superlattices) of octadecanethiol and octanethiol protected silver clusters has been studied with x-ray powder diffraction (XRD), differential scanning calorimetry (DSC), and infrared (IR) spectroscopy. These solids have been compared with the silver thiolate layered compounds in view of their similarity in alkyl chain packing and x-ray diffraction patterns. Superlattice melting is manifested in XRD around 400 K as the complete disappearance of all the low angle reflections; only bulk silver reflections due to the cluster cores are seen at 423 K. The superlattice structure is regained upon cooling from a temperature close to its melting point. However, cooling from a higher temperature of 473 K does not regain the superlattice order, whereas thiolate melting is repeatedly reversible even at these temperatures. Transmission electron microscopy suggests aggregation of clusters during heating/cooling cycles. DSC shows two distinct transitions, first corresponding to alkyl chain melting and the second corresponding to superlattice melting. Only alkyl chain melting is observed in variable temperature IR and increased order is manifested upon repeated heating/cooling cycles. Alkyl chain assembly shows strong interchain coupling leading to factor group splitting in cluster superlattices upon annealing. In thiolates only one melting feature is seen in DSC and it produces gauche defects, whereas significant increase in defect structures is not seen in superlattices. Repeated heating/cooling cycles increase interchain interactions within a cluster and the superlattice order collapses. © 2000 American Institute of Physics. [S0021-9606(00)70245-5]

## INTRODUCTION

Quantum dot (QD) superlattices have been of immense interest in the recent past due to the diverse properties possible in these systems.<sup>1-3</sup> Assembly of semiconductor<sup>2</sup> and metal QDs<sup>3</sup> has been observed in transmission electron microscopy of thin films. Monolayer protected metal clusters<sup>4</sup> are ideal systems to make such superlattices in three dimensions. In the course of our investigations of self-assembled monolayers (SAMs) grown on planar surfaces by surface enhanced Raman<sup>5</sup> and x-ray photoelectron spectroscopies,<sup>6</sup> a decision was made to look at the three dimensional monolayers grown on metal clusters. This enabled the investigation of structure and properties of the monolayer systems by a large number of techniques. Following the reports of superlattices in transmission electron microscopic (TEM)<sup>7</sup> and small angle x-ray scattering (SAXS)<sup>8(a)</sup> investigations, we refined our synthetic approach for the preparation of single-phase superlattice solids. These solids have been probed by a range of techniques such as x-ray diffraction (XRD), transmission electron microscopy (TEM), Fourier transform infrared spectroscopy (FT-IR), x-ray photoelectron spectroscopy (XPS), UV-VIS, nuclear magnetic resonance spectroscopy

(NMR), mass, thermogravimetry (TG), differential scanning calorimetry (DSC), and conductivity studies.<sup>9</sup> In this paper, we focus on the melting of the superlattice solids. Phase transitions of Ag nanocrystal superlattices have been investigated before<sup>8</sup> as a function of the ratio,  $\langle L \rangle/R$  between the capping ligand chain length with the core nanocrystal radius.<sup>8(a)</sup> While face centred cubic (fcc) packing was seen for  $\langle L \rangle/R < 0.60$ , body centered cubic (bcc) was favored for  $\langle L \rangle/R > 0.60$ . When  $\langle L \rangle/R > 0.66$ , body centered tetragonal packing was seen in octanethiol capped clusters.<sup>8(a)</sup>

The crystalline solids investigated here are not superlattices in the conventional sense since no appropriate sublattice exists. They can be described better as crystalline solids of monolayer protected clusters. The metal atoms and the monolayers within a cluster possess translational periodicity, as in the bulk metal and in the alkane solid, respectively. We refer to them as superlattices to be consistent with the literature reports.<sup>7</sup>

Alkyl chain assembly in planar SAMs is closely related to that in layered silver thiolates.<sup>10</sup> Extensive investigations of monolayer protected clusters suggest that the alkyl chain assembly in them is similar to monolayers on planar surfaces.<sup>4</sup> Thus it is likely that the molecular assembly of monolayer covered cluster solids is related to that of layered thiolates. This comparison is all the more meaningful since

<sup>a)</sup> Author to whom correspondence should be addressed. Electronic mail: pradeep@iitm.ac.in

many structural and spectroscopic insights into the structure of cluster solids can be derived from the comprehensive studies of thiolates.<sup>10</sup> Pioneering study of Dance *et al.*<sup>10(a)</sup> suggested that the alkyl chains in an all-*trans* orientation are projected in either direction from a layered Ag–S lattice to make layered silver thiolates. Detailed x-ray diffraction and transmission infrared spectroscopic investigations of Parikh *et al.*<sup>10(b)</sup> have shown that small interpenetration of the layers exist which results in the formation of one dimensional corridors, which alternate between the layers. The thiolate solids show mesogenic behavior after melting, in all except the ethyl derivative.<sup>10(c)</sup> The alkyl chain assembly need not be all-*trans*, as revealed by Fijolek *et al.*<sup>10(d)</sup> Their structural and spectroscopic study of variously synthesized butanethiolates showed that the chain conformation changes all the way from all-*trans* to *gauche*, with a conformationally mixed phase in-between. The comprehensive study of Bensebaa *et al.*<sup>10(e)</sup> compared the alkyl chain assembly of thiolates with that of planar monolayers and monolayer protected clusters.

Our investigations are principally concerned with octanethiol and octadecanethiol protected silver cluster superlattices. Melting of these polycrystalline superlattice solids is probed by variable temperature XRD, FT–IR, and DSC. We compared the cluster superlattices with the corresponding silver thiolate layered solids through a number of experiments. These comparisons became necessary because apart from the reasons mentioned above, both the solids show similar, but not identical, XRD and IR features, which prompted us to suspect decomposition of clusters into thiolates.

## EXPERIMENT

**Materials:** Silver nitrate (Merck, 99.99%), chloroauric acid (HAuCl<sub>4</sub>·3H<sub>2</sub>O, CDH, 99.8%), tetra *n*-octyl ammonium bromide (Merck, 98%), sodium borohydride, octadecanethiol, octanethiol (all Aldrich, 99%) were used as received. Toluene and methanol used were of AR grade. In all these syntheses, deionized and subsequently distilled water was used.

**Synthesis:** Octadecane and octane thiol protected clusters were synthesized using a modified literature method described originally for gold clusters.<sup>11</sup> These will be referred to later as C18 (Ag–ODT) and C8 (Ag–OT) clusters, respectively. Briefly, 0.0358 M toluene solution (21.6 ml) of tetra *n*-octyl ammonium bromide was added to a vigorously stirred 0.0288 M aqueous solution (10 ml) of AgNO<sub>3</sub>. After 1 hour of stirring, a 0.0139 M toluene solution (23.8 ml) of the respective thiol was added. To this, 8.25 ml aqueous solution (0.2378 M) of sodium borohydride was added dropwise. Reduction and derivatization of silver was manifested by the brown color of the toluene phase, which was originally colorless. The solution was stirred overnight and the organic layer was separated. It was allowed to evaporate slowly to 10 ml (this took several hours to a few days at the ambient temperature) and 100 ml of methanol was added in order to precipitate the cluster. The precipitate was allowed to settle and was collected by centrifuging. The material was washed several times with methanol to remove unreacted thiol and was air dried. The product obtained was a fine brown powder. Purity of the sample was ascertained by

NMR. The synthetic procedures were performed at 298 K. The materials were stored in ambient laboratory air and no significant change in the spectroscopic properties were observed in the time scale of two months. We observed that the solubility of the samples decreases with time, possibly due to aggregation, which was studied by UV-VIS.<sup>9</sup> Heated samples are not soluble in toluene, also due to aggregation (see below).

Silver thiolate layered materials were prepared by a modified literature procedure.<sup>10(e)</sup> A 0.0139 M toluene solution (47.6 ml) of the respective thiol was added to 0.0288 M aqueous solution (20 ml) of AgNO<sub>3</sub> while stirring and the resulting solution was stirred for 3 hours. A white suspension was formed in the toluene phase. Aqueous layer was found to be free of Ag<sup>+</sup>. Precipitate in the toluene phase was collected by centrifuging, washed with toluene and air dried. Due to the possible light sensitivity of these materials, all syntheses were performed in covered flasks and the materials were stored in brown colored bottles.

The superlattice solids have been thoroughly characterized by various techniques such as TEM, XRD, FT–IR, TG, DSC, UV-VIS, NMR, XPS, and mass spectrometry.<sup>9</sup> However, the present studies are focused on XRD, DSC, and FT–IR and only those experimental details are given below.

**X-ray diffraction:** X-ray diffractometers with CuK $\alpha$  or CoK $\alpha$  radiations were used for room temperature measurements. The samples were spread on antireflection glass slides to form uniform films. The films were wetted with acetone for uniformity and were blown dry before the measurement (use of acetone did not have any effect, confirmed with pressed pellets). All samples were similarly prepared. For variable temperature measurements, an X' Pert-MPD diffractometer with CuK $\alpha$  radiation was used. The sample was spread on a tantalum heating plate and at each temperature, the sample was allowed to stabilize for 3 minutes and the diffractogram in the range of 3°–51° (2 theta) was measured. A step size of 0.05° was used. Note that several measurements were performed on the same sample. The data were acquired rapidly due to the potential x-ray induced damage of RS<sup>-</sup> species.<sup>12</sup> Due to this the spectral quality was inferior to that of normal single scan measurements. Thiolates and a few superlattice solids were studied with a Siemens diffractometer using CuK $\alpha$  radiation. Data in the range of 2°–70° were measured in the temperature range of 303–423 K, at every 20 K interval. A step size of 0.02° was used.

**Infrared spectroscopy:** Infrared spectra were measured with a Bruker IFS 66v FT–IR spectrometer. Samples were prepared in the form of pressed KBr pellets. All spectra were measured with a resolution of 4 cm<sup>-1</sup> and were averaged over 200 scans. Variable temperature measurements were performed with a home-built heater and a programmable temperature controller.

**Differential scanning calorimetry:** DSC data were taken with a Netzsch PHOENIX DSC204 instrument. 10 mg of the samples encapsulated in aluminum pans was used. The measurements were conducted in the temperature range of 123–473 K. Thermogravimetric measurements showed that there is no weight loss in this temperature window and thiolate desorption commences only above 540 K in these samples.

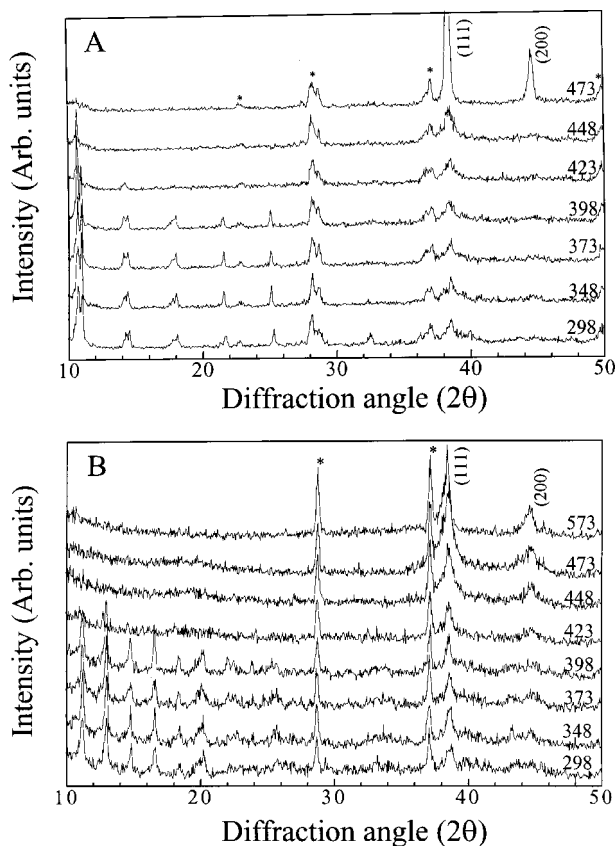


FIG. 1. Variable temperature x-ray ( $\text{CuK}\alpha$ ) powder diffraction patterns of (A) Ag-OT and (B) Ag-ODT. The temperatures are marked in the figure. The isolated silver cluster reflections are marked, these are immediately noticeable in the topmost diffractogram of (A). The peaks labeled with asterisks (\*) are due to the heating base plate. Due to possible x-ray induced damage of the thiolates, the spectra were acquired rapidly.

Repeated heating/cooling experiments were performed with the same sample. Separate measurements were performed to confirm the reproducibility of the data.

There are distinct differences between superlattice solids and thiolates, as discussed in the Appendix.

## RESULTS

The sections are divided into two pertaining to phase transition of superlattices and thiolates.

### Melting of superlattices

*Variable temperature x-ray diffraction:* Earlier studies have shown that Ag clusters of average core diameter  $4.0 \pm 0.5$  nm capped with alkanethiols form single-phase superlattice solids.<sup>9</sup> The x-ray powder diffractograms of these solids show low-angle peaks, which can be fully indexed to single cubic unit cells.<sup>9</sup> Whereas alkanethiols with five or more carbon atoms form superlattices, the corresponding cluster with four carbons yield only separated clusters identical to the three dimensional self-assembled monolayers investigated before.<sup>4,13</sup> No superlattice reflections are seen with the corresponding gold clusters.

Figure 1 shows the *in situ* variable temperature x-ray powder diffraction patterns of Ag-OT (A) and Ag-ODT (B). In order to make a comparison of the data, the intensities were not manipulated for presentation except for the offset,

for clarity. As can be seen, the room temperature patterns show low angle reflections. The bulk silver reflections are at  $38.48^\circ$  and  $44.60^\circ$ , which are observed in Ag-ODT [Fig. 1(B)]. In Ag-OT [Fig. 1(A)] note the absence of any intensity at  $44.60^\circ$  in the room temperature spectrum due to the bulk (200) reflection, suggesting that the material is essentially single-phase superlattice<sup>9</sup> (see also below). This means that the peak at  $38.59^\circ$  may also be attributable to the superlattice. All the low angle reflections at  $10.87^\circ$ ,  $14.43^\circ$ ,  $17.99^\circ$ ,  $21.69^\circ$ ,  $25.33^\circ$ , and  $32.60^\circ$  in Ag-OT [Fig. 1(A)] can be fully indexed to a simple cubic unit cell of  $a = 59.172 \text{ \AA}$ . Note that the patterns also show some lines due to the heating base plate, which are marked with asterisks (\*). The Ag-ODT pattern can be assigned to a simple cubic unit cell of  $a = 67.465 \text{ \AA}$ . The superlattice reflections are observed up to a temperature of 398 K and the diffractogram at this temperature is not different from that at room temperature. We do not see any shift in the peak positions and there is no emergence of additional peaks up to this temperature indicating the absence of phase transitions in the material. Diffractograms at 423 K show the near complete disappearance of the superlattice reflections and at 448 K the isolated cluster reflections begin to increase in intensity. In the data at 473 K, the (111) and (200) reflections of Ag have increased in intensity. Beyond 473 K, the pattern is essentially unchanged; data are presented for Ag-ODT at 573 K. Upon cooling down (from the highest temperature), the superlattice reflections are absent and there is no change in the (111) and (200) reflections of silver (not shown). This suggests that the material does not regain the superlattice order upon cooling. We will come back to this aspect later in the paper. It appears that the cluster core anneals, which results in the increase in the intensity of the Ag lattice reflections.

The data presented show that the superlattice is stable up to 398 K. It is important to see that there appears to be no large difference in the transition temperature for the two chain lengths. Upon increasing the temperature to 473 K and subsequently cooling down, the system becomes an orientationally disordered glass showing no superlattice reflections but only isolated Ag cluster pattern. In order to see whether it is possible to regain the superlattice after melting, the sample was immediately cooled after the collapse of the superlattice. In Fig. 2, we show a series of such experiments performed on the same sample. The diffraction patterns of Ag-ODT upon heating to different temperatures and cooling to 303 K (*in situ* in the diffractometer) are presented here. When the sample was heated to 423 K and subsequently cooled back, the superlattice reflections are still observed. The superlattice is also seen for the sample, which was cooled back from 448 K. However, these reflections are completely absent upon heating to 473 K and cooling back [Fig. 2(f)].

One of the interesting aspects to note is that the superlattice reflections are much narrower than the isolated cluster reflections. The particle size of the superlattices from the Scherrer formula<sup>14</sup> works out to be  $239 \text{ \AA}$ , although the effective core size of the cluster from TEM is of  $40 \text{ \AA}$ , indicating that each particle is composed of many superlattice unit cells.<sup>9</sup> However, the particle size of isolated clusters is

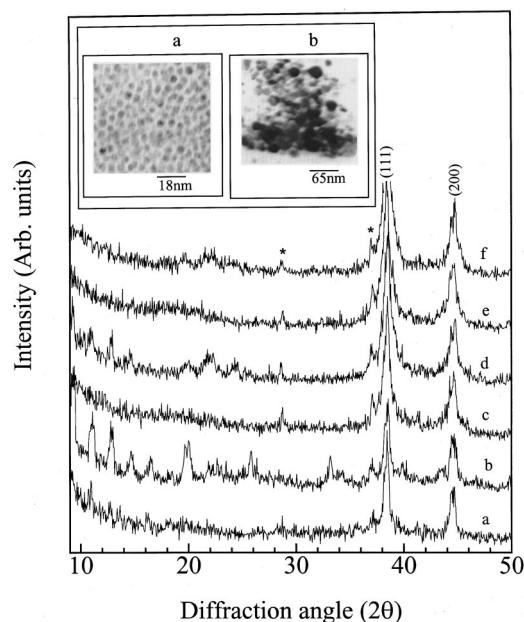


FIG. 2. X-ray powder diffraction ( $\text{CuK}\alpha$ ) profiles of Ag-ODT at various temperatures. (a), (c), and (e) correspond to the patterns at 423, 448, and 473 K, respectively. (b), (d), and (f) are the patterns at 308 K upon cooling the sample from 423, 448, and 473 K, respectively. All the experiments were performed on the same sample (i.e., the sample was cycled between the high temperature and 308 K). The peaks labeled with asterisks (\*) are due to the heating base plate. Inset shows TEM of (a) Ag-OT superlattice solid and (b) the same after heating to 473 K.

much smaller, for example, that corresponding to the top curve of Fig. 2. In gold clusters where superlattice is not seen in XRD, the Scherrer formula values are close to the cluster dimensions obtained from TEM. In Au-ODT, TEM gives a core diameter value of  $3 \pm 0.5$  nm and the Scherrer formula value is 29 Å. The inset of Fig. 2 shows the TEM of (a) superlattice solid and the (b) sample after heating to 473 K. The TEM of the *superlattice solid*, although shows a high degree of uniformity of particle size ( $4 \pm 0.5$  nm), no regular order is observed. However, a *drop cast film of the cluster* shows periodic order.<sup>9</sup> We explain this as due to the melting of the solid under electron beam, note that these solids are principally hydrocarbon assembled materials. We have seen that large crystallites melt and flow immediately upon exposure to the electron beam. In (b) the clusters got aggregated, which prevents the formation of superlattice upon cooling.

**Differential scanning calorimetry:** In Fig. 3 we compare the differential scanning calorimetric data of Ag-ODT under three experimental conditions. The sample was heated initially to 423 K from 123 K and was allowed cool to 298 K (experiment 1). It was then reheated to 423 K and again allowed cool to 298 K (experiment 2). In experiment 3 the sample was heated to 473 K and then cooled to 298 K. Data were collected in all three experiments. The DSC traces show two transitions, the first around at 339.7 K and another at 399.2 K, the former is due to the melting of the alkyl chain assembly and the second is due to that of the superlattice (see below). In Au-ODT, the peak temperature of the first transition is 333.5 K. We attribute the higher transition temperature in the case of Ag-ODT to the presence of the superlattice, which resulted in an increase in interchain interactions.

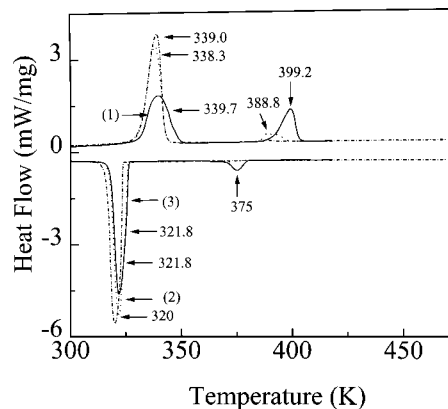


FIG. 3. (A) Differential scanning calorimetric traces of Ag-ODT upon repeated heating and cooling cycles. Three separate cycles are shown by the lines (1) (—), (2) (···), (3) (---). (1) Heating to 423 K and cooling back, (2) repeat of the same and (3) heating to 473 K and cooling back. In all the experiments, a heating/cooling rate of 10 K/min was used. All the experiments pertain to one sample. Transition temperatures and enthalpies are given in Table I.

The enthalpy of superlattice melting (Table I) is substantial, which indicates that the cohesive energy of the super structure is high. A molecular dynamics study<sup>15</sup> of the alkanethiolate capped gold superlattice predicts a cohesive energy of 15 eV/cluster. Upon cooling the solid from 423 K, the transitions are again manifested; the superlattice freezing enthalpy is considerably less than the melting. The alkyl freezing, however, releases more energy, presumably because of the annealing of defects. In addition, the clusters may act as nucleating sites for crystallization.

In experiment 2, both the transitions are seen in either direction; the enthalpies of both are roughly the same as in the first cooling experiment. Upon cooling, the superlattice freezing is observable (Table I, not clear in the figure), but the enthalpy has substantially reduced. Enthalpy of alkyl freezing is comparable to the value of melting. In experiment 3 upon warming, both the transitions are observed; the energetics of the first is comparable to that of the previous experiment. The superlattice melting is observed but the enthalpy has reduced significantly. Upon cooling, freezing of the superlattice is not observed at all.

TABLE I. Enthalpies and transition temperatures of the octadecanethiolate capped silver cluster superlattice from DSC upon repeated heating/cooling cycles.

	Ag-ODT			
	$\Delta H_1$ (J/g)	$T_1$ (K)	$\Delta H_2$ (J/g)	$T_2$ (K)
Heating from 123 K to 423 K	107.9	339.7	46.3	399.2
Cooling from 423 K to 123 K	136.4	321.8	9.4	375.0
Heating from 298 K to 423 K	139.5	338.3	13.4	388.8
Cooling from 423 K to 298 K	153.0	321.8	1.3	371.1
Heating from 298 K to 473 K	149.5	339.0	1.5	388.9
Cooling from 473 K to 298 K	163.0	320.0		

Both XRD and DSC show the reversibility of the superlattice transition at lower temperatures and irreversibility at higher temperatures. Thus, the XRD and DSC results are in perfect agreement with each other. The results suggest that the molten superlattice has two distinctly different forms, one in which the alkyl chains can reform just as in the original solid and in the higher temperature phase, the alkyl chains lose memory of the original order and cooling results in a disordered phase of isolated clusters. The increase in alkyl chain melting enthalpy upon repeated heating/cooling cycles is significant. One obvious reason could be the annealing of the defects in the alkyl chain order. Variable temperature infrared investigations have shown that the alkyl chains have attained increased order upon cooling (see below).

To compare the behavior with the corresponding Au systems, an experiment was performed with Au-ODT. Here again, both transitions are observed. In accordance with the XRD data, where no superlattice reflections were observed, the superlattice melting enthalpy was found to be low, indicating that the fraction of material in this state is less. Note that while the superlattice melting enthalpy is about 43% of the alkyl melting energy in Ag-ODT, it is only 4.5% in Au-ODT. The alkyl melting goes through multiple phases unlike in the case of Ag-ODT, probably due to the interdigitation of individual monolayer chains. Upon cooling down (from 473 K), the superlattice freezing is not seen, but the individual steps of alkyl freezing are observable. Just as in the case of Ag, enthalpy increases upon cooling due to the annealing of defects.

A corresponding DSC experiment was performed for Ag-OT. The data were measured as in the case of Ag-ODT (see above). The superlattice melting occurred gradually in the first heating and there is almost continuous absorption of energy although there are three distinct maxima at 377.0, 382.9, and 388.6 K, which are seen in subsequent heating experiments also. This behavior appears to be associated with the interdigitated alkyl chains. Upon cooling, two distinct superlattice-freezing transitions are seen; the enthalpies are lower than the melting. The superlattice melting enthalpy in second heating is comparable to that of the first freezing and three distinct transitions are observed. The superlattice melting temperature reduces slightly with decrease in chain length. Unlike in the case of Ag-ODT where there was a distinct temperature corresponding to the superlattice melting, Ag-OT shows several transition temperatures. Upon first heating, almost continuous absorption of energy is manifested. It seems that several conformations of the alkyl chains got frozen in the superlattice solid of Ag-OT, whereas the alkyl chain order appears to be similar to an alkane crystal in the case of Ag-ODT resulting in a sharper transition (see below).

**Variable temperature infrared spectroscopy:** In order to find an explanation for the observed behavior and to understand the nature of alkyl chain order, a variable-temperature infrared investigation was performed. In Fig. 4, we show the temperature-dependent FT-IR spectra of Ag-ODT in the range of 298 K to 473 K. The C-H stretching and low-frequency regions are shown separately [in (A) and (B), re-

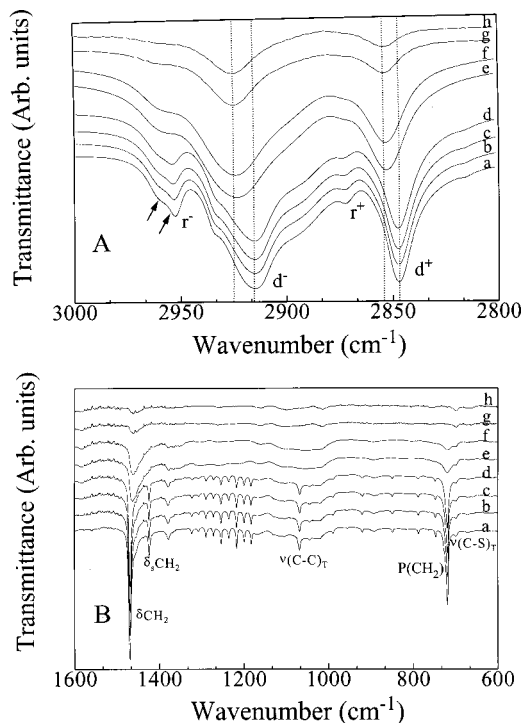


FIG. 4. Variable temperature FT-IR spectra of Ag-ODT. (A) and (B) corresponds to the C-H stretching and low frequency regions, respectively. Spectra were measured in KBr matrices. The temperatures are (a) 298, (b) 323, (c) 348, (d) 373, (e) 398, (f) 423, (g) 448, and (h) 473 K.

spectively]. Positions of the methylene vibrations can be taken as a measure of the order (crystallinity) of the alkyl chains. In the case of crystalline polyethylene, the frequencies of the symmetric ( $d^+$ ) and antisymmetric ( $d^-$ )  $\text{CH}_2$  modes are at 2846–2849 and 2916–2918  $\text{cm}^{-1}$ , respectively.<sup>16</sup> The values blueshift to 2856 and 2928  $\text{cm}^{-1}$  in liquid.<sup>16(c)</sup> This increase corresponds to greater number of gauche defects. For 2D SAMs, crystalline-like behavior is found for chain lengths above C6.<sup>17</sup> Here the  $d^+$  and  $d^-$  modes appear at 2848 and 2919  $\text{cm}^{-1}$ , respectively, clearly suggesting all-*trans* conformation. Similar positions are seen in the case of 3D SAMs on Au.<sup>18</sup> The  $r^+$  (symmetric) and  $r^-$  (antisymmetric) bands of the methyl group for all alkanethiolates lie at almost similar values of 2868 and 2957  $\text{cm}^{-1}$ , respectively, throughout. The  $r^-$  band is composed of at least two components as marked in the Fig. 4. To make two asymmetric  $\text{CH}_3$  vibrations degenerate, the methyl group should possess at least  $C_3$  symmetry. This symmetry is not present in the alkyl chain assembly, as chains are nonequivalent. This asymmetry arises due to the intermolecular interactions between the adjacent alkyl chains. Since the peaks are not well resolved, although observable clearly, we suggest that the chain ends undergo hindered rotation. Thus limited orientational freedom exists for the chain termini. All the other bands can be assigned on the basis of *n*-alkane vibrations and have been discussed in detail before.<sup>9</sup> At room temperature, the  $d^+$  and  $d^-$  modes appear at 2847 and 2915  $\text{cm}^{-1}$ , respectively, characteristic of crystalline alkanes, indicating solidlike order. These modes shift to 2853 and 2924  $\text{cm}^{-1}$ , respectively, at 398 K; the values are those of liquid alkanes.<sup>16(c)</sup> A drastic shift corresponds to the melting of the

alkyl chain. It is important to see that the phase transition temperature (398 K) is higher than the value reported for Au clusters.<sup>19</sup> Note that the transition temperature observed in IR is significantly higher than that seen in DSC, as noted by Badia *et al.*<sup>19</sup> At the transition temperature, the  $r^-$  modes merge and shift to a higher value. This also indicates total rotational freedom of the alkyl chains.

In the low frequency region, the positions of all the bands, and especially the presence of the wagging and the rocking progression bands suggest the presence of crystalline alkyl chains. The assignments are fully described in earlier papers. Prior to the melting transition, the  $\delta_s\text{CH}_2$  mode (assigned to the scissoring mode of the methylene close to the cluster surface) at  $1421\text{ cm}^{-1}$  begins to shift and broaden. At the melting temperature, the transition becomes so broad that it is not observable, indicating that the alkyl chain as a whole attains rotational freedom and consequently the lifetime of the vibrational state decreases. The  $\delta\text{CH}_2$  mode at  $1468\text{ cm}^{-1}$  shows only broadening, but no shift. The broadening of these two peaks is significant since it indicates the occurrence of additional channels of relaxation for the entire alkyl chain, which is mostly free rotation. A corresponding effect is seen on the methylene rocking mode ( $\text{P}(\text{CH}_2)$ ) at  $720\text{ cm}^{-1}$ . At  $323\text{ K}$  the  $\nu(\text{C}-\text{C})_T$  appearing at  $1068\text{ cm}^{-1}$  shows a downshift and at the monolayer melting temperature, the band disappears completely. We attribute the redshift in the frequency to increased order or annealing of the chains. Note that only  $\nu(\text{C}-\text{C})_T$  shows redshift, not  $\nu(\text{C}-\text{H})$  or  $\delta\text{CH}_2$ . An increase in the alkyl chain melting temperature is suggested to be a signature of the superlattice. The fact that the superlattice is stable even after heating the solid above the monolayer melting transition implies that intercluster interaction is significant.

Melting of the alkyl chains and the formation of liquid like structure are also evidenced by a number of other signatures. The C-C stretching and the progression bands disappear completely. Although the  $\text{CH}_2$  wagging band close to the cluster surface ( $\delta_s\text{CH}_2$ ) labeled in Fig. 4(B) loses intensity completely, there is still some intensity for the wagging band corresponding to the other  $\text{CH}_2$  groups. The presence of rotational freedom is also clear. At the same time, the C-H and the C-S stretching modes are present in the molten state, showing that the alkyl chains are still adsorbed on the surface. Note that the  $(\text{C}-\text{S})_G$  mode at  $698\text{ cm}^{-1}$  is retaining the intensity throughout while all the other peaks decrease in intensity. Note especially the decrease in intensity of the  $720\text{ cm}^{-1}$  band due to  $\text{P}(\text{CH}_2)$  and  $\nu(\text{C}-\text{S})_T$ . In fact this peak completely disappears above  $448\text{ K}$ . This would suggest that after melting the conformation around C-S is essentially gauche. Note that the C-S mode does not show any shift during the experiment, indicating that the nature of binding is unaffected.

The sample upon heating and subsequent cooling was examined in separate experiments (in pure state, not in KBr matrix). The FT-IR spectra of Ag-ODT shown in Fig. 5 were recorded at  $298\text{ K}$ , for the following sets of conditions: (a) as prepared, (b) following heating to  $398\text{ K}$  and subsequent cooling to  $298\text{ K}$ , (c) following heating to  $473\text{ K}$  and subsequent cooling to  $298\text{ K}$ . The C-H stretching and low

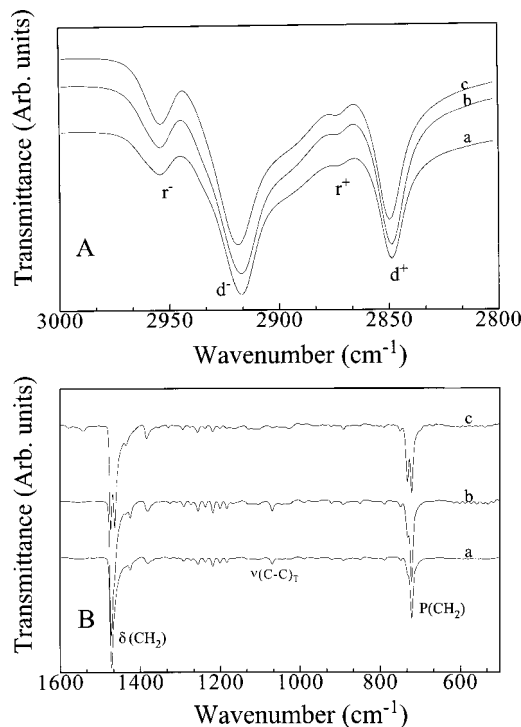


FIG. 5. FT-IR spectra of Ag-ODT in the (a) as prepared condition, (b) after heating to  $398\text{ K}$  and subsequent cooling to  $298\text{ K}$ , and (c) after heating to  $473\text{ K}$  and subsequent cooling back to  $298\text{ K}$ . Fresh samples were used for each heating and cooling experiment. The spectra were measured in KBr matrices. (A) and (B) correspond to CH stretching and low frequency regions, respectively.

frequency regions are plotted in (A) and (B). The  $d^+$  and  $d^-$  modes appear approximately at the same energy (within  $2\text{ cm}^{-1}$ ) indicating that the alkyl chains are crystalline in all the samples. However, in spectrum (c), there is a substantial reduction in the peak width, which is particularly noticeable for the  $r^-$  mode at  $2953\text{ cm}^{-1}$ . This is attributed to the annealing of the defects in the alkyl chain assembly. This increased order is visible in the  $\delta\text{CH}_2$  mode, resolved into two peaks at  $1463$  and  $1473\text{ cm}^{-1}$  of almost equal intensity in spectrum (c). These two peaks are attributable to factor group splitting in the monoclinic unit cell and is observed in the infrared spectra of many hydrocarbon crystals.<sup>20</sup> In the temperature dependent IR spectra of monolayers, the methylene scissoring mode splits into two at  $80\text{ K}$ , which has been attributed to increased order in the alkyl chain assembly.<sup>21</sup> In spectrum (b), the  $\delta\text{CH}_2$  mode has a shoulder corresponding to the emergence of a new peak. As a result of annealing, the methylene-rocking mode at  $720\text{ cm}^{-1}$  is split into two peaks of almost similar intensity at  $720$  and  $730\text{ cm}^{-1}$ . An identical splitting of the rocking mode is found in pure hydrocarbon crystals and is suggested to be due to the in-phase vibrations of adjacent, differently oriented, alkyl chains in the monoclinic unit cell.<sup>20,22</sup> All of these signatures are indicative of increase in the alkyl chain order, which is in perfect agreement with the DSC results. Au-ODT behaves similarly, although the factor group splitting is not as distinct as in Ag-ODT.

Similar experiments are performed on Ag-OT cluster superlattices also. The methylene ( $\text{CH}_2$ ) symmetric ( $d^+$ )

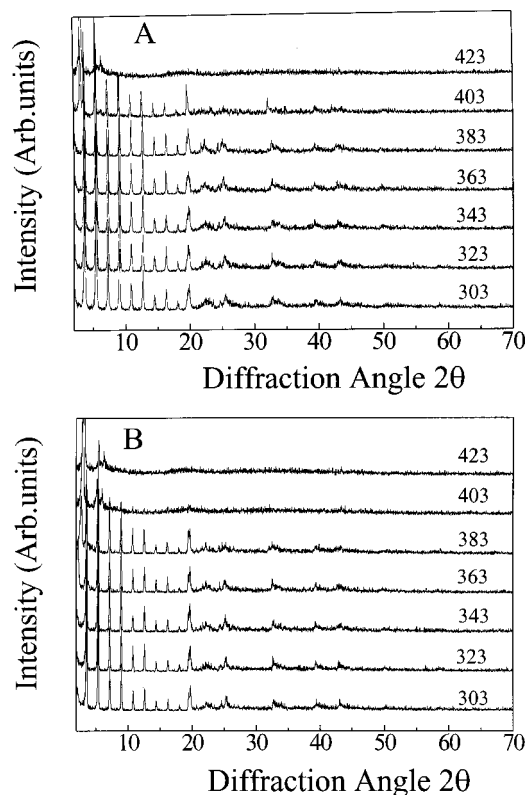


FIG. 6. Variable temperature XRD pattern of the Ag-octadecanethiolate (A) while heating and (B) while cooling. Temperatures are marked in the figure. All the reflections came back after cooling.

and antisymmetric ( $d^-$ ) modes appear at 2847 and 2916  $\text{cm}^{-1}$ , at room temperature, respectively, are characteristic of crystalline alkanes,<sup>16</sup> indicating the solidlike order. These modes shift to 2852 and 2923  $\text{cm}^{-1}$ , at 378 K, values indicative of liquid alkanes.<sup>16(c)</sup> Melting is manifested in the progression bands also. All the bands undergo reduction in intensity and become broad during the transition. The  $\nu\text{C}-S_T$  mode got reduced in intensity and become equal to that of the  $\nu\text{C}-S_G$  at 398 K.

### Melting of thiolates

In this section we present data pertaining to Ag-octadecanethiolate. The data of Ag-octanethiolate is similar.

**Variable temperature x-ray diffraction:** In order to see the melting of thiolates, we have performed variable temperature XRD measurements on these samples as well. In Fig. 6(A) the XRD pattern of Ag octadecanethiolate during heating is shown. At 423 K, most of the low angle reflections disappeared as in the case of the superlattice. As expected, the bulk Ag reflections at  $38.48^\circ$  and  $44.60^\circ$  are not emerging at this temperature. Studies of Baena *et al.*<sup>10(c)</sup> have established that the crystalline phase transforms to a micellar phase at 404.4 K. The micellar phase is a hexagonal columnar mesophase and the micellar→amorphous phase transition occurs at 448.0 K. While cooling down from 423 K [Fig. 6(B)] the micellar phase reverts to the parent crystalline phase below 403 K and the diffraction pattern at 383 K is identical to that of the starting material, suggesting the total reversibility of the transition.

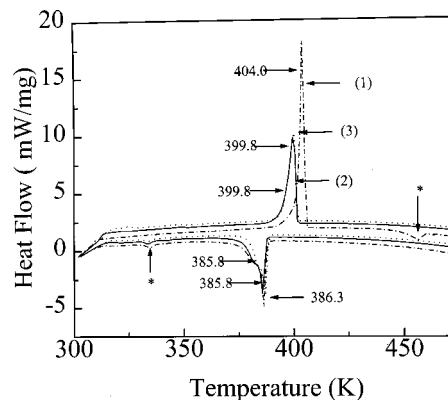


FIG. 7. Differential scanning calorimetric traces of Ag-octadecanethiolate upon repeated heating/cooling cycles. Three cycles are shown by the lines (1) (---), (2) (—), (3) (···). Transition temperatures are marked in the figure. The transition is reversible even after three heating cycles, unlike in Fig. 3. Asterisks (\*) show instrumental fluctuations.

**Differential scanning calorimetry:** In Fig. 7 the DSC traces of Ag-octadecanethiolate are shown. *Only one transition* (at 404.0 K) is observed, which is different from the superlattices. Three cycles of heating/cooling were performed (marked separately) and it can be seen that even after heating to 473 K, the transition is *repeatedly reversible*. While cooling down a two-step transition is observed, possibly due to the various mesogenic phases<sup>10(c)</sup> possible. In the superlattices, we saw that the melting transition is reversible only if it is heated up to 423 K. Also note the larger enthalpy changes compared to the superlattice. After the first heating, all the energy values are almost identical, in sharp contrast with the superlattice data.

**Variable temperature infrared spectroscopy:** Figure 8 shows the variable temperature IR spectra of the (A) high and (B) low frequency regions of Ag-octanethiolate layered solids. The methylene ( $\text{CH}_2$ ) symmetric ( $d^+$ ) and antisymmetric ( $d^-$ ) modes appear at 2847 and 2918  $\text{cm}^{-1}$  respectively, which is characteristic of crystalline alkanes,<sup>16</sup> indicating the solidlike order. These modes shift to 2853 and 2923  $\text{cm}^{-1}$  at 393 K, values which correspond to those of liquid alkanes.<sup>16(c)</sup> Melting is manifested in the progression bands also. All the bands undergo reduction in intensity and become broad during the transition. Formation of  $\nu(\text{C}-S)_G$  after the transition indicates that during the transition gauche defects were increased. The transition is at a higher temperature than that of the superlattices, which indicates that the van der Waals attraction is stronger in the case of thiolates.

### COMPARISON BETWEEN SUPERLATTICES AND THIOLATES

For a better appreciation of the differences between the superlattice and the thiolate, the room temperature XRD data of Ag-OT superlattice and Ag-octanethiolate are presented in Fig. 9. These data were acquired with improved statistics. Note that the superlattice solid was repeatedly washed with toluene to remove isolated clusters, which are freely soluble. The immediate difference we see is the number of additional reflections seen in the thiolate, particularly at higher diffraction angles. The superlattice reflections gradually shift in the

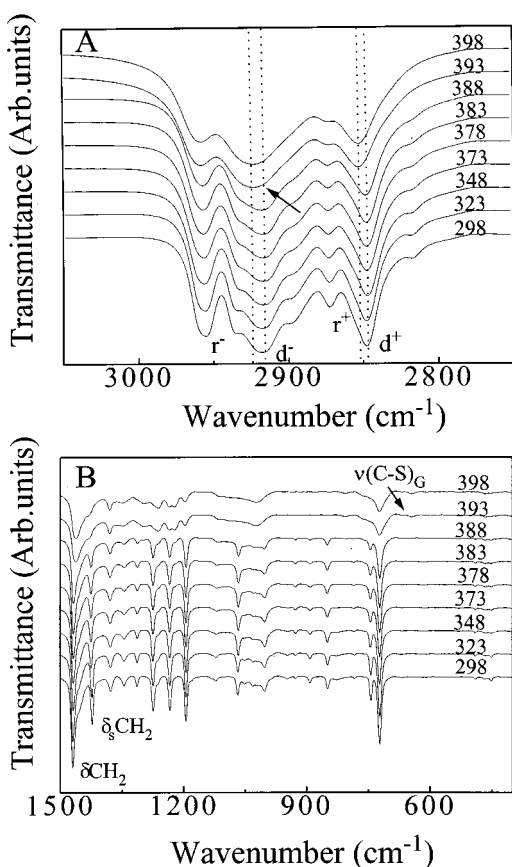


FIG. 8. Variable temperature IR spectra of Ag-octanethiolate layered solids, (A) high frequency region and (B) low frequency region. Temperatures (in Kelvin) are marked in the figure. Note that the transition temperature is higher than that in Fig. 4. The drastic shift in the  $d^-$  mode (A) upon melting is marked. The appearance of  $\nu(\text{C-S})_G$  upon melting is indicated (B).

negative direction as the diffraction angle is increased (see the inset). This shows the larger interplanar distance in the superlattice compared to the thiolate. Doubling of the superlattice reflections are seen, probably due to some distortion in the structure. The superlattice pattern also shows the bulk (111) reflection of Ag. The large number of higher angle peaks due to intralayer reflections is not seen in the superlattice.

IR spectra show distinct differences between the superlattices and thiolates. The  $\nu\text{C-S}_G$  at  $669\text{ cm}^{-1}$  in the Ag-OT cluster is absent in the thiolate at room temperature, which indicates all *trans* conformation without any defects in the latter. Moreover, all the progression bands are well formed in the thiolate as reported in the literature<sup>10(b)</sup> whereas they are not as pronounced in the superlattice. C-H region also exhibits distinct differences; while the bands are broad in the thiolate they are narrower in the cluster. The intensity ratio of  $d^-/r^-$  is less in thiolate, which shows that the first two or three methylene groups do not contribute to the intensity of  $d^-$ . The IR intensity ratio  $I_{2920}/I_{2850}$  can be taken as a measure of disorder,<sup>16</sup> and with the increase in conformational order, this ratio decreases. In the case of thiolates the ratio is lesser compared with that of cluster. This indicates that thiolates are more ordered. The difference between the two solids is further seen in the phase transition. The multiple step

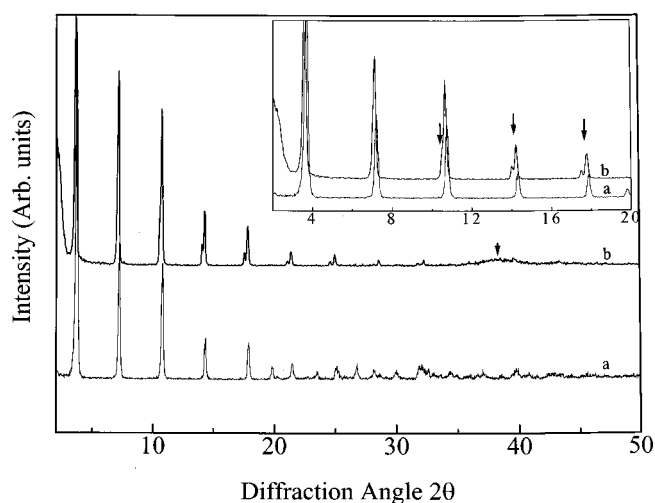


FIG. 9. Room temperature XRD patterns of (a) Ag-octanethiolate and (b) Ag-OT superlattice. Inset shows the expanded region of the same showing the differences between the two. The splitting is marked in the figure. Note the increasing shift between the two at higher angles. The (111) reflection of bulk Ag in (b) is indicated by an arrow. The data were taken with improved statistics.

transition of Ag-OT superlattice in DSC is quite different from Ag-octanethiolate, which shows only a sharp single transition at 403.3 K. Superlattice transition becomes irreversible at 473 K, whereas, even after heating to 473 K, the transition is repeatedly reversible in thiolates. Factor group splitting of methylene scissoring and rocking modes upon annealing was observed in superlattices, whereas it was absent in thiolates.

## DISCUSSION

The superlattice unit cell dimension increases from 59.172 in Ag-OT to 67.465 Å in Ag-ODT. The increase in the lattice parameter is 8.293 Å for an increase of 10 carbon atoms in the alkyl chain body. Upon increasing the number of carbon atoms in the alkyl chain body from five in the pentanethiol protected silver cluster to eight in Ag-OT, the unit cell dimension increases by 6.149 Å.<sup>9</sup> If interdigitation is occurring between separated alkyl chains, the extent to which it occurs has to be greatly different in different samples to explain the experimental facts, which is quite unlikely. Also such a structure may have resulted in a large increase in superlattice melting temperature with increase in alkyl chain length. Thus it appears that the superlattices are formed principally as a result of interdigitation of bundles of monolayers assembled on the cluster surfaces. The fact that Ag-OT shows multiple superlattice melting transitions implies that there could be more conformations of the chains contributing to the superlattice assembly. A greater penetration of bundles with increasing chain length also increases packing density. This argument is also supported by the fact that alkyl chain order is similar to that existing in 2D and 3D monolayers.

It is seen that between successive heating and cooling (in Ag-ODT), the temperature of the alkyl chain melting is not changing. However, the width of the transition narrows and the enthalpy increases. This suggests that the kind of order is

similar in both as prepared and temperature cycled samples but there is a significant amount of defects in the parent sample and these defects are removed upon subsequent heating/cooling cycles. The increase in alkyl chain melting enthalpy is not seen in isolated Au clusters,<sup>19(a)</sup> whereas there is a significant decrease in enthalpy for the superlattice solid. It is possible that the superlattice acts as nucleation sites in acquiring alkyl chain order. It is possible that there are a number of alkyl chains in the superlattice solid occupying the edges and terraces of the cluster surface which are not perfectly ordered, but could do so upon annealing contributing to the increased enthalpy upon cooling.

The superlattice melting enthalpy reduces upon repeated cycling. In other words, although alkyl chain order increases, the superlattice assembly collapses during annealing. Thus, a superlattice of the clusters is possible only if there are significant defects in the monolayer order of the isolated clusters. As these defects are annealed out, leading to perfect all-*trans* order within each of the planes of the cluster surface, the superstructure becomes less probable. It is possible that heating/cooling cycling also causes changes in the morphology of the cluster surface, which helps in removing the defects.

As the superstructure is formed from the solution phase, it is possible that a few of the alkyl chains are not ordered. The lack of order can be a result of geometric constraints in the superlattice structure or due to the presence of defect sites at the cluster surface as mentioned earlier. Upon allowing the molten alkyl chains to cool, the van der Waals forces between the chains of individual molecules dominate over those between the clusters, thus increasing the number of superlattice unit cells that separate.

Why the superlattice state especially that of Ag-ODT, exhibits two distinct liquid phases is an interesting question. In the phase below 448 K, the liquid can regain the superlattice order, whereas above 473 K, liquid is unable to retrieve the superlattice order. It is unlikely that in such a small temperature difference, the cluster core acquires sufficient energy for a large displacement from its equilibrium position. It is more likely that the alkyl chain acquires another orientation which does not permit the superlattice order. However, this structure leads to a more complete order for the monolayer upon cooling, which results in a higher monolayer freezing enthalpy. This can happen due to either (1) structural changes in the cluster or (2) conformational changes in the alkyl chain body. We do not have much evidence for (1) from spectroscopy; however, observed aggregation has to involve structural changes. The fact that a few of the modes are narrowing and resolving upon annealing indicates that conformational differences are being removed. This indicates that the superlattice structure requires some degree of defects in the alkyl chain body. Thus, it is clear that the superstructure is not formed from isolated ordered clusters but instead both superlattice and the isolated clusters evolve in a single precipitation step. This suggests that solution phase growth is preferred for superlattice formation. The temperature cycling does result in increased crystallinity of the cluster core as seen by the enhancement of the (111) and (220) reflections at higher temperature; however, this does not change the nature

of alkyl chain binding. The effect of cluster core annealing on the conformational changes in the alkyl chain assembly is unknown.

## CONCLUSIONS

Superlattices of alkanethiol capped silver clusters melt above 398 K after the melting of the alkyl chain monolayer. There is a small, but significant reduction in melting point upon decreasing the chain length. Repeated cycles of heating and cooling remove the defects in the alkyl chain body and the fraction of superlattice decreases. The superlattice melting is manifested in variable temperature XRD as the complete loss of the low angle reflections and with the emergence of separated Ag cluster reflections. DSC shows two distinct transitions, the first corresponding to the alkyl chain melting and the second corresponding to the superlattice melting whereas in thiolates, only one transition is observed. The superlattice melting proceeds through several steps in clusters of lower chain length. Variable temperature IR spectroscopy shows distinct signatures only for the alkyl chain melting and not for superlattice melting. In thiolates, only one distinct melting transition is seen in IR corresponding to the collapse of the lattice. It is concluded that a perfect alkyl chain order within the isolated clusters is not necessary for the superlattice structure.

## ACKNOWLEDGMENTS

T.P. thanks the Department of Science and Technology, Government of India and Council of Scientific and Industrial Research, Government of India for financial support. N.S. thanks the Council of Scientific and Industrial Research, Government of India, for a research fellowship.

## APPENDIX

*Physical properties of cluster superlattices and thiolates:* While superlattice solids are dark brown, thiolates are white crystalline powders. No change in color was seen during the period of the experiment. The superlattice solids are completely soluble in nonpolar solvents, whereas the thiolates are insoluble under identical conditions. The solubility of the cluster sample decreased upon storage (in air). To see whether this is due to the degradation of cluster to thiolate, a number of experiments were performed. The insoluble and soluble portions were separated and all the measurements were conducted on both samples. In both cases, the superlattice signatures were observed and the absorption spectra of the solutions as well as the solids were characteristic of the clusters. There was no thiolate feature<sup>10(e)</sup> in the UV/VIS (thiolate shows a distinct absorption peak with a sharp edge at 320 nm). It was ascertained through independent experiments that the large absorbance of the cluster did not mask the thiolate feature. The solubility of Ag-OT and Ag-ODT clusters (in nonpolar organic solvents) just after complete reduction (the material was in the organic phase) was checked. They were completely soluble. After 12 hours of stirring, the solubility in toluene was checked again, and complete solubility was seen. If thiolate is forming along with the cluster during the preparation, we should get an

insoluble fraction. Absence of the same suggests solely the formation of clusters. Other possibility is that the thiolate (which may have formed) is incorporated onto the cluster surface, which makes this thiolate soluble. In that case, they could separate during precipitation. Considering the possibility of slow kinetics involved in such phase separations, one portion of the cluster solution (soon after preparation) was kept at low temperature (278 K) and another was kept at room temperature. After one week both the samples were completely soluble in toluene. The solutions were evaporated slowly. After complete evaporation, the cluster was completely redissolved in toluene. Later methanol was added to precipitate the cluster and soon after precipitation, the sample could be redissolved completely. All these observations suggest that the material synthesized is pure cluster superlattice.

To see whether thiolate, possibly formed initially, can be reduced to become clusters, a thiolate suspension was reacted with a solution of  $\text{NaBH}_4$  as in the cluster synthesis. It was found that the thiolate could not be reduced effectively at room temperature. However, upon increasing the temperature to 353 K, some reduction occurred, as indicated by the change in color of the solution, but almost all of the material was insoluble upon cooling to room temperature. The precipitate showed characteristic signatures of thiolate in XRD and UV-VIS.

In order to see whether the cluster is intercalated in thiolate, a suspension of Ag octanethiolate in toluene was refluxed separately at two temperatures, 343 K and 393 K. Even though the thiolate is not soluble at room temperature, it forms a homogeneous solution at 333 K. Ag-OT cluster solution in toluene was added to both the flasks and refluxing at these temperatures was continued for 12 h. While cooling down to room temperature, the thiolate precipitated completely, whereas Ag-OT cluster was in solution. The absorption spectrum of the solid showed both the thiolate absorption (edge at 320 nm [Ref. 10(a)]) and a weak plasmon excitation (at 520 nm, shifted from the solution phase value at 430 nm due to solid-state effects).<sup>9</sup> Note that we did not observe any thiolate absorption in our superlattice solids or cluster solutions. XRD shows the same thiolate reflections at exactly the same positions, which indicates the absence of intercalation and subsequent lattice expansion. This is in accordance with the report of Dance *et al.*,<sup>10(a)</sup> who attempted intercalation of organic molecules in thiolates. It appears that a small portion of clusters could be adsorbed on thiolates, which contributes to the absorption spectrum. Since the extinction coefficient of plasmon absorption is large, it is easily observable. All these experiments ruled out the possibility of thiolate in the superlattice solid. There are also distinct differences in XRD, IR, and DSC of the two solids (*vide supra*).

<sup>1</sup>C. P. Collier, T. Vossmeier, and J. R. Heath, *Annu. Rev. Phys. Chem.* **49**, 371 (1998); G. Springholz, V. Holy, M. Pinczolis, and G. Bauer, *Science* **282**, 734 (1998).

<sup>2</sup>T. Vossmeier, G. Reck, L. Katsikas, ETK. Haupt, B. Schulz, and H. Weller, *Science* **267**, 1476 (1995); P. C. Ohara, D. V. Leff, J. R. Heath, and W. Gelbert, *Phys. Rev. Lett.* **75**, 3466 (1995); R. L. Whetten, J. T. Khoury, M. M. Alvarez, S. Murthy, I. Vezmar, Z. L. Wang, C. C. Cleve-

land, W. D. Ludtke, and U. Landman, *Adv. Mater.* **8**, 428 (1996); R. P. Andres, J. D. Bielefeld, J. I. Henderson, D. B. Janes, V. R. Kolagunta, C. P. Kubiak, W. J. Mahoney, and R. G. Osifchin, *Science* **273**, 1690 (1996); M. J. Hostetler, S. J. Green, J. J. Stokes, and R. W. Murray, *J. Am. Chem. Soc.* **118**, 4212 (1996).

<sup>3</sup>N. Herron, J. C. Calabrese, W. Farneth, and Y. Wang, *Science* **259**, 1426 (1993); C. B. Murray, C. R. Kagan, and M. G. Bawendi, *ibid.* **270**, 1335 (1995).

<sup>4</sup>See for a review, M. J. Hostetler and R. W. Murray, *Curr. Opin. Colloid Interface Sci.* **2**, 42 (1997).

<sup>5</sup>N. Sandhyarani, K. V. G. K. Murty, and T. Pradeep, *J. Raman Spectrosc.* **29**, 359 (1998); N. Sandhyarani and T. Pradeep, *Vacuum* **49**, 279 (1998); N. Sandhyarani, G. Skanth, S. Berchmans, V. Yegnaraman, and T. Pradeep, *J. Colloid Interface Sci.* **209**, 154 (1999); K. V. G. K. Murty, M. Venkataramanan, and T. Pradeep, *Langmuir* **14**, 4446 (1998); M. Venkataramanan, G. Skanth, K. Bandyopadhyay, K. Vijayamohan, and T. Pradeep, *J. Colloid Interface Sci.* **212**, 553 (1999); M. Venkataramanan, T. Pradeep, W. Deepali, and K. Vijayamohan, *Langmuir* (in press); K. Bandyopadhyay, K. Vijayamohan, M. Venkataramanan, and T. Pradeep, *ibid.* **15**, 5314 (1999).

<sup>6</sup>V. Bindu, A. Dorothy, and T. Pradeep, *Int. J. Mass Spectrom. Ion Processes* **155**, 69 (1996); V. Bindu and T. Pradeep, *Vacuum* **49**, 63 (1998); V. Bindu, M. Venkataramanan, and T. Pradeep, *Mol. Phys.* **96**, 367 (1999).

<sup>7</sup>J. R. Heath, C. M. Knobler, and D. V. Leff, *J. Phys. Chem. B* **101**, 189 (1997); S. A. Harfenist, Z. L. Wang, M. M. Alvarez, I. Vezmar, and R. L. Whetten, *J. Phys. Chem.* **100**, 13904 (1996); Z. L. Wang, *Adv. Mater.* **10**, 13 (1998).

<sup>8</sup>(a) B. A. Korgel and D. Fitzmaurice, *Phys. Rev. B* **59**, 14191 (1999); (b) N. Sandhyarani, T. Pradeep, J. Chakrabarti, M. Yousuf, and H. K. Sahu, *ibid.* **62**, R739 (2000).

<sup>9</sup>N. Sandhyarani, M. R. Resmi, R. Unnikrishnan, S. Ma, K. Vidyasagar, M. P. Antony, G. Panneer Selvam, V. Visalakshi, N. Chandrakumar, K. Pandian, Y.-T. Tao, and T. Pradeep, *Chem. Mater.* **12**, 104 (2000).

<sup>10</sup>(a) I. G. Dance, K. J. Fisher, R. M. Herath Bamda, and M. L. Scudder, *Inorg. Chem.* **30**, 183 (1991); (b) A. N. Parikh, S. D. Gillmor, J. D. Beers, K. M. Beardmore, R. W. Cutts, and B. I. Swanson, *J. Phys. Chem.* **103**, 2850 (1999); (c) M. J. Beana, P. Espinet, M. C. Lequerica, and A. M. Levelut, *J. Am. Chem. Soc.* **114**, 4182 (1992); (d) H. G. Fijolek, J. R. Grohal, J. L. Sample, and M. J. Natan, *Inorg. Chem.* **36**, 622 (1997); (e) F. Bensebaa, T. H. Ellis, E. Kruus, R. Voicu, and Y. Zhou, *Langmuir* **14**, 6579 (1998).

<sup>11</sup>S. R. Johnson, S. D. Evans, S. W. Mahon, and A. Ulman, *Langmuir* **13**, 51 (1997).

<sup>12</sup>See, for example, V. L. Colvin, A. N. Goldstein, and A. P. Alivisatos, *J. Am. Chem. Soc.* **114**, 5221 (1992).

<sup>13</sup>M. Brust, M. Walker, D. Bethell, D. J. Schiffrin, and R. Whyman, *J. Chem. Soc. Chem. Commun.*, 801 (1994); R. H. Terril, T. A. Postlethwaite, C.-H. Chen *et al.* *J. Am. Chem. Soc.* **117**, 12537 (1995); M. Brust, J. Fink, D. Bethell, D. J. Schiffrin, and C. Kiely, *J. Chem. Soc. Chem. Commun.*, 1655 (1995); D. V. Leff, L. Brandt, and J. R. Heath, *Langmuir* **12**, 4723 (1996); D. V. Leff, P. C. Ohara, J. R. Heath, and W. M. Gelbart, *J. Phys. Chem.* **99**, 7036 (1995); M. M. Alvarez, J. T. Khoury, T. G. Schaaff, M. N. Shafiqullin, I. Vezmar, and R. L. Whetten, *J. Phys. Chem. B* **101**, 3706 (1997).

<sup>14</sup>A. R. West, *Solid State Chemistry and its Applications* (Wiley, New York, 1987).

<sup>15</sup>W. D. Luedtke and U. Landman, *J. Phys. Chem.* **100**, 13323 (1996).

<sup>16</sup>(a) R. A. MacPhail, H. L. Strauss, R. G. Snyder, and C. A. Elliger, *J. Phys. Chem.* **88**, 334 (1982); (b) M. Maroncelli, S. P. Qi, H. L. Strauss, and R. G. Snyder, *J. Am. Chem. Soc.* **104**, 6237 (1982); (c) R. G. Snyder, H. L. Strauss, and C. A. Elliger, *J. Phys. Chem.* **86**, 5145 (1982).

<sup>17</sup>M. D. Porter, T. B. Bright, D. L. Allara, and C. E. D. Chidsey, *J. Am. Chem. Soc.* **109**, 3559 (1987).

<sup>18</sup>M. J. Hostetler, J. J. Stokes, and R. W. Murray, *Langmuir* **12**, 3604 (1996).

<sup>19</sup>(a) A. Badia, S. Singh, L. Demers, L. Cuccia, G. R. Brown, and R. B. Lennox, *Chem. Eur. J.* **2**, 359 (1996); (b) A. Badia, L. Cuccia, L. Demers, F. Morin, and R. B. Lennox, *J. Am. Chem. Soc.* **119**, 2682 (1997).

<sup>20</sup>R. G. Snyder, *J. Mol. Spectrosc.* **7**, 116 (1961); J. R. Nielsen and C. E. Hathaway, *ibid.* **10**, 366 (1963).

<sup>21</sup>L. H. Dubois and R. G. Nuzzo, *Annu. Rev. Phys. Chem.* **43**, 437 (1992).

<sup>22</sup>N. B. Colthup, L. H. Daly, and S. E. Wiberley, *Introduction to Infrared and Raman Spectroscopy* (Academic, New York, 1975), p. 232.